

Composite dielectrics and conductors: simulation, characterization and design

D P Almond, C R Bowen and D A S Rees

Materials Research Centre and Bath Institute for Complex Systems, Department of Mechanical Engineering, University of Bath, Claverton Down, Bath BA2 7AY, UK

Received 22 June 2005, in final form 24 November 2005

Published 17 March 2006

Online at stacks.iop.org/JPhysD/39/1295

Abstract

Very large networks of randomly positioned resistors and capacitors have been used to simulate the microstructures of real two-phase (conductor–insulator) materials. These networks are found to exhibit fractional power law frequency dependences of dielectric properties and ac conductivity, of the type reported for a wide range of materials. The network results are related to the resistor and capacitor values by a simple logarithmic mixing rule. The same mixing rule is used to model the electrical characteristics of two-phase electrical composites. The results are tested using water impregnated lead zirconate titanate (PZT) ceramics samples that have a microstructure that forms a complex interconnected random array of conducting (water) and insulating regions. Excellent agreement is obtained between the experimental data and the modelling predictions based on the network simulation results. The power law exponents for ac conductivity and relative permittivity are found to be equal to the proportions of the composite occupied by the insulating and conducting phases, respectively. Studies of conducting polymer impregnated PZT are also presented which show less good agreement with modelling predictions.

1. Introduction

The development of electrical composites is motivated by the technological need for properties that are not available in individual single component materials. By combining two or more components it becomes possible to tailor composite materials with the required combinations of properties. The design of such electrical composites necessitates a detailed understanding of the ways in which composite properties depend upon component properties, composition and composite microstructure. Theoretical studies of heterogeneous dielectric materials have been in a continuous state of development since the initial work of Maxwell. The bulk of these studies have been based on utilizing exact solutions for geometrically simple (spheres, discs, cylinders etc) inclusions of one component in a continuous matrix formed by another component. These studies have resulted in a range of effective medium theories and in the determination of rigorous bounds on the predictive capabilities of particular models. A review of this large body of work has been made by Brosseau and Beroual [1]. In more recent years, a range of numerical modelling techniques have

been employed to study increasingly complex systems of inclusions, particularly randomized distributions of inclusions, in composites. The computational demands of this work are high because of the need to model large numbers of inclusions to ensure that the results are representative of the real macroscopic composite samples.

We offer here an alternative approach to composite design that has arisen from efforts to understand another longstanding problem: the anomalous power law frequency dependence of dielectrics [2–4]. Recently [5–8], we proposed that the anomalous power law dispersions of permittivity and ac conductivity, found in many materials, could be attributed to the electrical response characteristics of two-phase, conductor–insulator, networks formed by their microstructures. Microstructural examinations of many materials that exhibit these anomalous properties reveal complex random arrays of conducting and insulating/capacitive phases. We have suggested [6–8] that such microstructural networks can be modelled as large networks of randomly positioned resistors and capacitors. The electrical characteristics of these networks are found to closely resemble those of the large body of materials that exhibit the anomalous power law frequency dependences of permittivity

or ac conductivity. It was shown [5] that a simple formula, arising out of the network simulation studies, could be used to accurately predict the electrical properties of a two-component composite material.

The purpose of this paper is to expand on the previous work [5], in which the emphasis had been on testing the validity of the proposed model by creating and measuring a suitable composite. In this paper we explore further the predictive capabilities of the network simulation models and test these predictions using measurements of a range of different composites. The principal findings of the network simulation studies are summarized in section 2 of the paper and new 3D finite element simulation results are introduced. These results are used in section 3 to predict the electrical response characteristics of composites. In section 4, these predictions are tested experimentally using carefully chosen and well-characterized composite samples. Finally, in section 5 the results of the experiments and the simulations are discussed.

2. Network simulation characteristics

The electrical response characteristics of large networks of randomly positioned resistors and capacitors were initially [6,7] obtained using commercial circuit simulation software [9]. This work was followed [8] by the development of a rapid network reduction algorithm that enabled the statistical variation of responses from network to network to be examined. The results that are typical of those found in these simulation studies are shown in figure 1. Simulations of the frequency dependence of the ac conductivity obtained from 255 different random networks are shown in figure 1(a). Each network was a square network containing 512 components of which 60% were randomly sited 1 k Ω resistors and the remaining 40% were 1 nF capacitors. Very similar results were found [8] for networks containing 2048, 8192 and 32,768 components. The frequency dependences of the capacitances of the same collection of 512 component networks are shown in figure 1(b). In both figures, the response characteristics exhibit three clear regimes of behaviour. To discuss these, it is helpful to introduce a third figure, figure 1(c), which shows the variation with frequency of the admittances of the individual network components. Whilst the resistors have a frequency independent admittance, R^{-1} , the admittances of the capacitors rise as ωC , where ω is the angular frequency.

At low frequencies, where $\omega C \ll R^{-1}$, the capacitors can be regarded as open circuits elements and the electrical responses of the networks are dominated by the networks of resistors alone. At these frequencies, a wide band of frequency independent conductivities were obtained, figure 1(a). These correspond to the many different percolation paths across the randomly positioned resistors in the 255 different random networks. At higher frequencies where ωC approaches R^{-1} , however, all the network responses are seen to converge upon a common characteristic: a power law dispersion of conductivity with frequency. This common characteristic occupies at least two decades of frequency, roughly centred about the ‘characteristic frequency’, 159 kHz, at which $\omega C = R^{-1}$ for the components used in the network simulations. The power law dispersion evident in figure 1(a) has an exponent of 0.4 ± 0.037 that matches the proportion of the network,

40%, occupied by capacitors. It has been pointed out [8] that this power law dispersion is an ‘emergent property’ of these networks, i.e. a well-defined characteristic of the electrical response that appears to be independent of the random arrangement of the resistors and capacitors in the networks. At these intermediate frequencies both component types make significant contributions to the overall electrical conduction of a network. Then, at high frequencies, where $\omega C \gg R^{-1}$, a broad band of conductivities returns. At these frequencies, capacitor admittances are so high that they short out much of the resistor network. However, as only 40% of the networks were occupied by capacitors there were insufficient number of them that could percolate the 2D square networks. It has been shown mathematically [10,11] that the percolation threshold for a 2D ‘bond’ lattice, of the type simulated here, is 50%. Consequently, at high frequencies the conductivities of the conduction paths across all the networks are limited by the inclusion of one or more resistors and it is their conductivities that determine the network response. Similar arguments can be used to explain the three regimes of behaviour of the network capacitances shown in figure 1(b).

The intermediate frequency range, power law response characteristics of the networks have been found [6–8] to follow a simple logarithmic mixing rule expression that is also known as Lichtenecker’s rule [12]. The complex conductivity, or admittance, of a network is found to conform with

$$\sigma_{\text{net}}^* = (i\omega C)^n (R^{-1})^{1-n}, \quad (1)$$

in which n is the proportion of the network that is occupied by the capacitors. The ac conductivities of the networks have magnitudes and frequency dependences that match the real part of equation (1):

$$\sigma_{\text{net}} = C^n R^{n-1} \cos(n\pi/2)\omega^n. \quad (2)$$

The imaginary part of equation (1) corresponds to the admittance, $i\omega C_{\text{net}}$, of the network. Hence the network capacitance is given by

$$C_{\text{net}} = C^n R^{n-1} \sin(n\pi/2)\omega^{n-1}. \quad (3)$$

The power law dispersion evident in figure 1(b) has an exponent of -0.6 that matches, in magnitude, the proportion of the network, 60%, occupied by resistors, and its amplitude is in good agreement with that predicted by equation (3).

The rationale for studying the properties of large networks of randomly positioned resistors and capacitors was that the microstructures of real materials could be seen to exhibit an array of randomly positioned and shaped resistive and capacitive phases. However, it is not clear that the above relationships obtained from studies of 2D networks should also apply to the 3D networks of interconnected phases formed by the microstructures of real materials. A comprehensive investigation of the characteristics of 3D networks has shown that the emergent power law relationships are a common feature of both 2D and 3D networks. A sample of this work, which will be published in full elsewhere, is presented here in figure 2. Figure 2 shows the results of 25 simulations of the network conductivities of $20 \times 20 \times 20$ element networks in which 50% of the elements, the A elements, were randomly

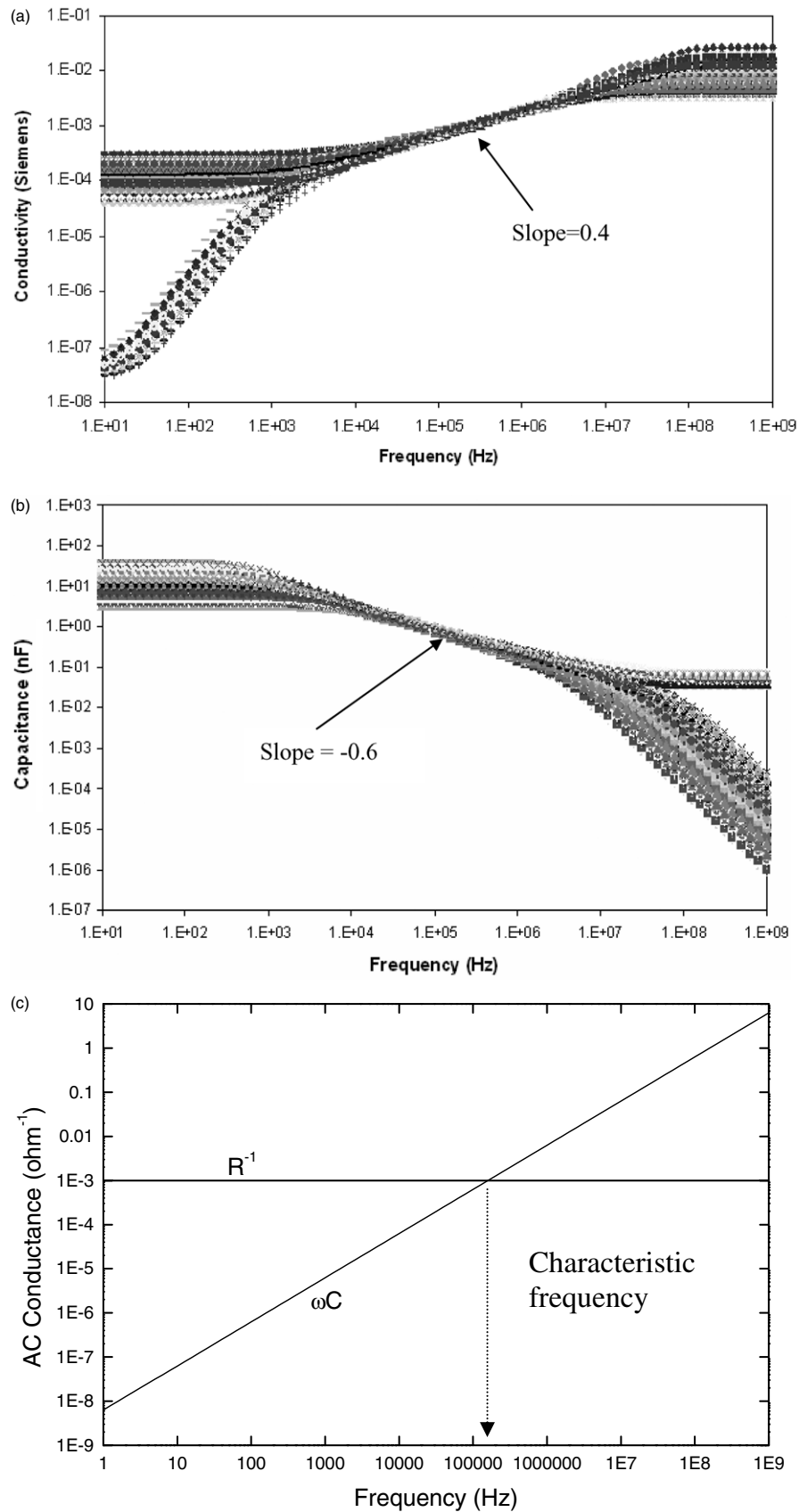


Figure 1. Network simulation frequency dependences [20] of (a) conductivity and (b) capacitance obtained for 255 networks containing 512 randomly positioned components of which 60% were $1\text{ k}\Omega$ resistors and 40% were 1 nF capacitors. (c) admittances of a $1\text{ k}\Omega$ resistor and a 1 nF capacitor across the same frequency range.

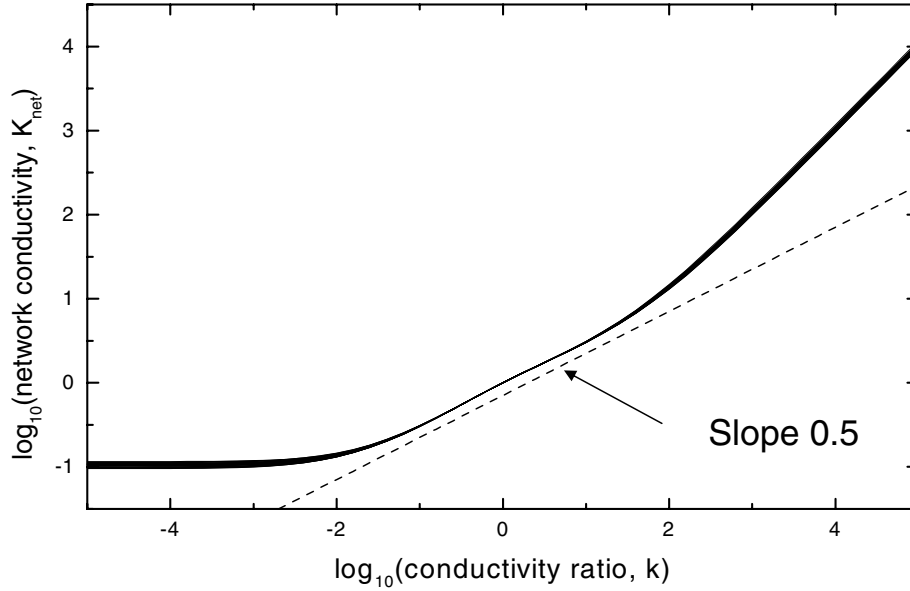


Figure 2. Finite element simulation dependences of bulk conductivity on the ratio of the conductivities of the two types of element. Results are shown for 25 simulations of a cube of $20 \times 20 \times 20$ elements with 50% of the element randomly chosen to have conductivities k , and the remainder assigned conductivity 1.

assigned a conductivity k whilst the remaining 50%, the B elements, were assigned a conductivity of 1. The figure shows the variations of network conductivity with k i.e. with the ratio of the conductivities of the two element types. The simulations were undertaken using a straightforward implementation of the method of successive over-relaxation to solve the full nodal equations in three dimensions.

Figure 1(c) provides the link between the independent variables, frequency and conductivity ratio employed in the 2D and 3D simulations. It is evident from figure 1(c) that as frequency is swept from low to high values, the ratio of the admittances, or ac conductivities, of the capacitors and resistors is swept from values $\ll 1$ to values $\gg 1$. Hence the frequency dependences of electrical network properties can be equated with the dependences of these properties on the ratio of the ac conductivities of the network components.

The 3D network characteristics, figure 2, exhibit the same three regimes of behaviour found in the 2D characteristics (figures 1(a) and (b)). At low conductivity ratios, $k \ll 1$, network conductivity is attributed to percolation paths along the B elements (conductivity 1) across the network. These elements occupy 50% of the networks whilst the percolation threshold for a 3D bond network is only 0.2492 [10]. At intermediate conductivity ratios, the characteristics converge on an emergent power law regime with a slope of 0.5, matching the proportion of the network occupied with the A elements having conductivity k . This regime is seen to occupy about four decades of conductivity ratio. Then at high conductivity ratios, $k \gg 1$, percolation on the A elements (conductivity k) dominates, leading to the regime with a slope of 1. The emergent power law part of the network characteristic is in good agreement with the logarithmic mixing rule for a system of two components having conductivities k and 1 in the proportions $n : (1 - n)$ i.e. the network conductivity is given by

$$K_{\text{net}} = k^n. \quad (4)$$

The great similarities between the results obtained in the 2D and 3D network simulations, in particular in the power law emergent regimes, gives us confidence in using the 2D electrical network expressions, equations (2) and (3), to predict the properties of real 3D composite materials.

To make the link to the network results it is necessary to associate the average conductivity of the resistive phases with that of a network resistor and the average capacitance of the capacitive phases with that of a network capacitor. This amounts to setting

$$R^{-1} = \sigma A/l \quad (5)$$

and

$$C = \varepsilon \varepsilon_0 A'/l', \quad (6)$$

where σ is the electrical conductivity of the resistive phase which, within the material, is taken to occupy, on average, regions of length l of cross-sectional area A . Similarly, ε is the relative permittivity of the capacitive phase that on average occupies regions length l' of cross sectional area A' . ε_0 is the permittivity of free space.

For the case in which the aspect ratios of the regions occupied by the two phases are equal, i.e. for $A/l = A'/l'$, substitution of expressions (5) and (6) in equations (2) and (3) yields simple formulae for the ac conductivity and relative permittivity of a two-phase composite material:

$$\sigma_{\text{comp}} = (\varepsilon \varepsilon_0)^n \sigma^{1-n} \cos(n\pi/2) \omega^n \quad (7)$$

$$\varepsilon_{\text{comp}} = \varepsilon^n \varepsilon_0^{n-1} \sigma^{1-n} \sin(n\pi/2) \omega^{n-1} \quad (8)$$

and the characteristics frequency becomes

$$f_{\text{ch}} = \sigma / (2\pi \varepsilon \varepsilon_0) \quad (9)$$

3. Model characteristics

It is generally recognized [4] that the ac conductivities and permittivities of a wide range of materials exhibit frequency dependences that are a reasonably good fit to expressions of the form

$$\sigma(\omega) = \sigma_{dc} + B\omega^p \quad (10)$$

$$\varepsilon(\omega) = D\omega^{p-1} + \varepsilon_{\infty}. \quad (11)$$

Equations (7) and (8) can be used to predict the frequency dependent parts of these expressions if the material is a composite containing two randomly distributed phases that are individually conducting and insulating and which satisfy the scaling relationship $A/l = A'/l'$. The latter condition would apply, for example, to composites having microstructures that could be modelled well by a lattice of equal size cubic elements—the phase of each element being randomly determined.

The dc conductivity, σ_{dc} , is determined by percolation paths across the material. It is evident that the network simulations, figures 1(a) at low frequencies, give no precise indication of percolation conductivity as at these frequencies conductivity is found to be highly variable between simulations, each having different percolation paths. A useful estimation of dc conductivity in porous solids, of the type investigated experimentally here, section 4, is Archie's law [13] that was obtained from measurements of the dc electrical conductivity of water-saturated rock

$$\sigma_{dc} = \sigma_{\text{water}} \cdot \phi^d, \quad (12)$$

where σ_{water} is the conductivity of the water, ϕ is the porosity level and d is a constant (typically ~ 2). More generally, equation (12) can be used to provide an estimate of dc conductivity due to percolation if the conductivity of the water is identified with the conductivity of the conducting phase, σ and the proportion of the material occupied by this phase, $(1 - n)$, is identified with ϕ and d is taken to be 2.

Whilst potential insulating materials, for use in electrical composites, exhibit a comparatively narrow range of relative permittivities (~ 2 – ~ 3000), potential conducting materials can have conductivities spanning ~ 12 orders of magnitude. However, it was noted above that the frequency dispersions were roughly centred on a characteristic frequency determined by the conducting and insulating properties of the two phases, equation (9). For practical reasons, the majority of ac response studies are made in the frequency range below ~ 10 MHz. If this frequency is set as the upper limit of characteristic frequency for materials of interest, it is found that conducting phases must have conductivities less than $\sim 1 \text{ Sm}^{-1}$. Metals have conductivities in the range $\sim 10^6$ – $\sim 5 \times 10^7 \text{ Sm}^{-1}$, at room temperature.

Model frequency dependences of ac conductivity are shown in figure 3 for composites comprising an insulating material with a relative permittivity, ε , of 10 occupying 60% by volume and randomly distributed conducting phases of conductivities indicated, occupying the remaining 40%. These curves were obtained by adding conductivity terms defined in equations (7) and (12) to provide an expression of the same form as equation (10). The shift in the onset frequency for the power law dispersion with the conducting phase conductivity

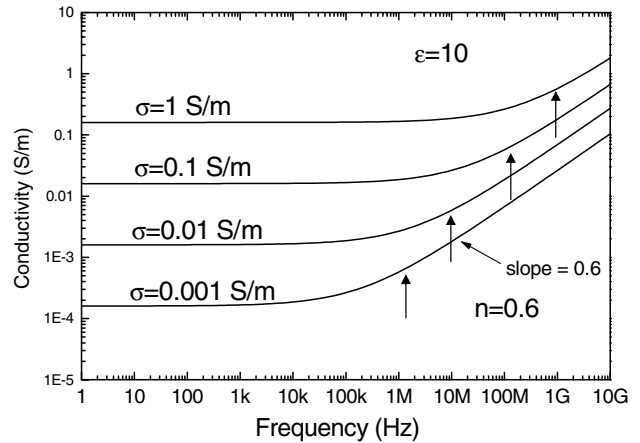


Figure 3. Modelling characteristics of the ac conductivity of a two-phase composite in which the insulating phase, relative permittivity 10, occupies 60% of the material and the conducting phase, with conductivities indicated, occupies the remaining 40%. Characteristic frequencies are indicated by the arrows.

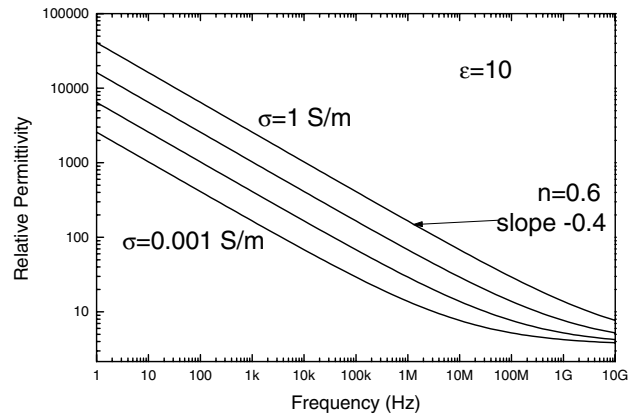


Figure 4. Modelling characteristics of the relative permittivity of a two-phase composite in which the insulating phase, relative permittivity 10, occupies 60% of the material and the conducting phase, with the same conductivities as shown in figure 3, occupies the remaining 40%.

is a consequence of the dependence of characteristic frequency on conductivity (equation (9)). The family of curves in figure 3 bears a striking resemblance to experimental data showing the variation of ac conductivity with temperature [4]. Many materials that exhibit such characteristics are effectively two-phase composites comprising a conducting phase, with a thermally activated conductivity, suspended within an insulating phase.

The model variations in relative permittivity with frequency for the same composites are shown in figure 4. These results were obtained using equation (8) to represent the frequency dependent term in equation (11). A permittivity of 3.25 was added to represent the permittivity ε_{∞} of a 40% porous sample [14] of the dielectric phase ($\varepsilon = 10$) at high frequencies, where the frequency dependent component of permittivity becomes negligible. The model predicts massive enhancements in relative permittivity and power law dispersions at low frequencies. The power law exponent has a magnitude, $(1 - n)$ from equation (8), equalling the proportion

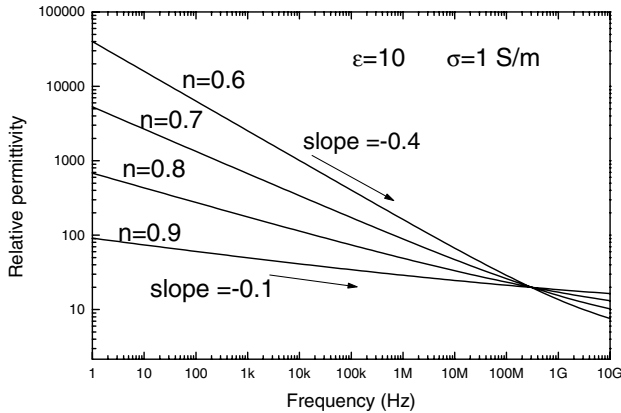


Figure 5. Modelling characteristics of the relative permittivity of a two-phase composite in which the insulating phase, relative permittivity 10, occupies the proportions n shown of the material with the conducting phase, conductivity indicated, occupying the remainder.

of the composite, here 0.4, occupied by the conducting phase. The frequency range of the power law dispersion shifts with conducting phase conductivity in a fashion similar to the dispersion in ac conductivity.

The model dependence of permittivity on composite composition is shown in figure 5. It can be seen that the characteristics form a fan of lines with slopes having magnitudes equalling the proportion of the composite occupied by the conducting phase. The effect of composition on conductivity is to cause the slope of the power law dispersion, equation (8), to be equal to the proportion of the composite occupied by the insulating phase. The effect of composition on permittivity is more distinctive than for conductivity because the added ϵ_{∞} term is insignificant in comparison with the permittivity power law term at low frequencies, whilst the reverse is the case for conductivities where σ_{dc} much exceeds the power law term.

4. Experimental results

The network simulation results, equations (7) and (8), have the same form as the experimental data obtained from a wide range of real materials, characterized by equations (10) and (11). In this section we present the results of experimental tests of the relevance of the simulation results to real materials.

The tests necessitate the selection of a composite that has a two phase, conductor–insulator, random microstructure and a characteristic frequency below ~ 10 MHz. In addition it is essential that the two phases can be characterized separately, prior to their incorporation as a composite.

The two materials selected to form the test system were the ferroelectric ceramic lead zirconate titanate (PZT), as the insulating/dielectric phase, and water as the conductive phase. PZT powder was sintered to form a low-density porous pellet that was infused with water. The pore structure of such a ceramic comprises a random 3D array of interconnected cavities that are readily filled with water. Interconnectivity (open porosity) and microstructure for these materials has previously been determined by the Archimedes method and microstructural analysis [14].

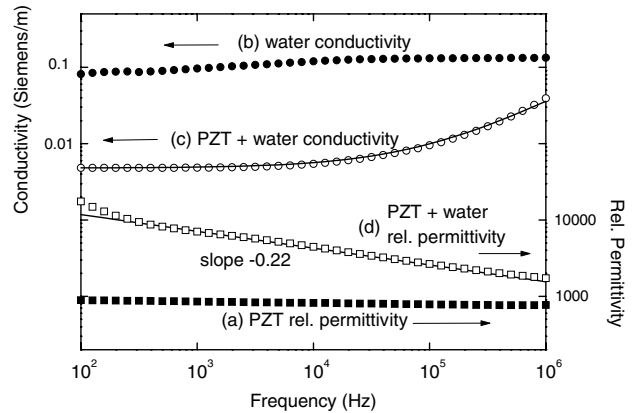


Figure 6. Measurements of (a) relative permittivity of a 22% porous PZT sample, (b) conductivity of water at equilibrium with immersed PZT fragments (see text), (c) the conductivity and (d) the relative permittivity of the sample saturated with water.

The major factor leading to the choice of water as the conducting phase was that it has an electrical conductivity $\sim 0.1 \text{ Sm}^{-1}$ that is required to set the characteristic frequency below 10 MHz. It also has the advantages of being readily available, of having fairly featureless dielectric characteristics in the frequency range of interest here and of being simple to introduce into the insulating host, in the manner mentioned above.

The first test sample was a sintered PZT pellet that had a diameter of 10.5 mm, a thickness of 3 mm and a density of 78% of the theoretical density (a porosity of 22%). Silver paste electrodes were applied to the two circular faces and electrical measurements were made using a Solartron 1260 impedance analyzer with a Solartron 1296 dielectric interface. The measured relative permittivity of the PZT sample, prior to the introduction of the water, is shown in figure 6(a). The permittivity is featureless across the frequency range shown, 100 Hz to 1 MHz, but has a magnitude of ~ 900 that is lower than that, 1500, for fully dense bulk PZT due to the presence of porosity in both series and parallel with the PZT through its thickness. The permittivity of materials with 22 vol% porosity, evaluated by modelling and experiment, is typically 50–60% that of the dense material [15–17].

The frequency dependence of the conductivity of the water is shown in figure 6(b). PZT ceramic fragments were immersed in the water sample for 70 h prior to the measurements to ensure that a good indication of the conductivity of the water within the pores of the ceramic was obtained. It was found that the pieces of ceramic raised the water conductivity by a factor of ~ 5 , presumably by dissolution of ionic impurity compounds on the ceramic surfaces. The conductivity of the water sample is flat and featureless across the frequency range shown with a small decrease at lowest frequencies attributable to an electrode polarization effect that is commonly observed in ac measurements of all types of ionic conductors [18].

The ac conductivity and relative permittivity of the porous PZT sample saturated with water are shown in figures 6(c) and (d). The experimental data for both the conductivity and permittivity are similar to the modelling predictions

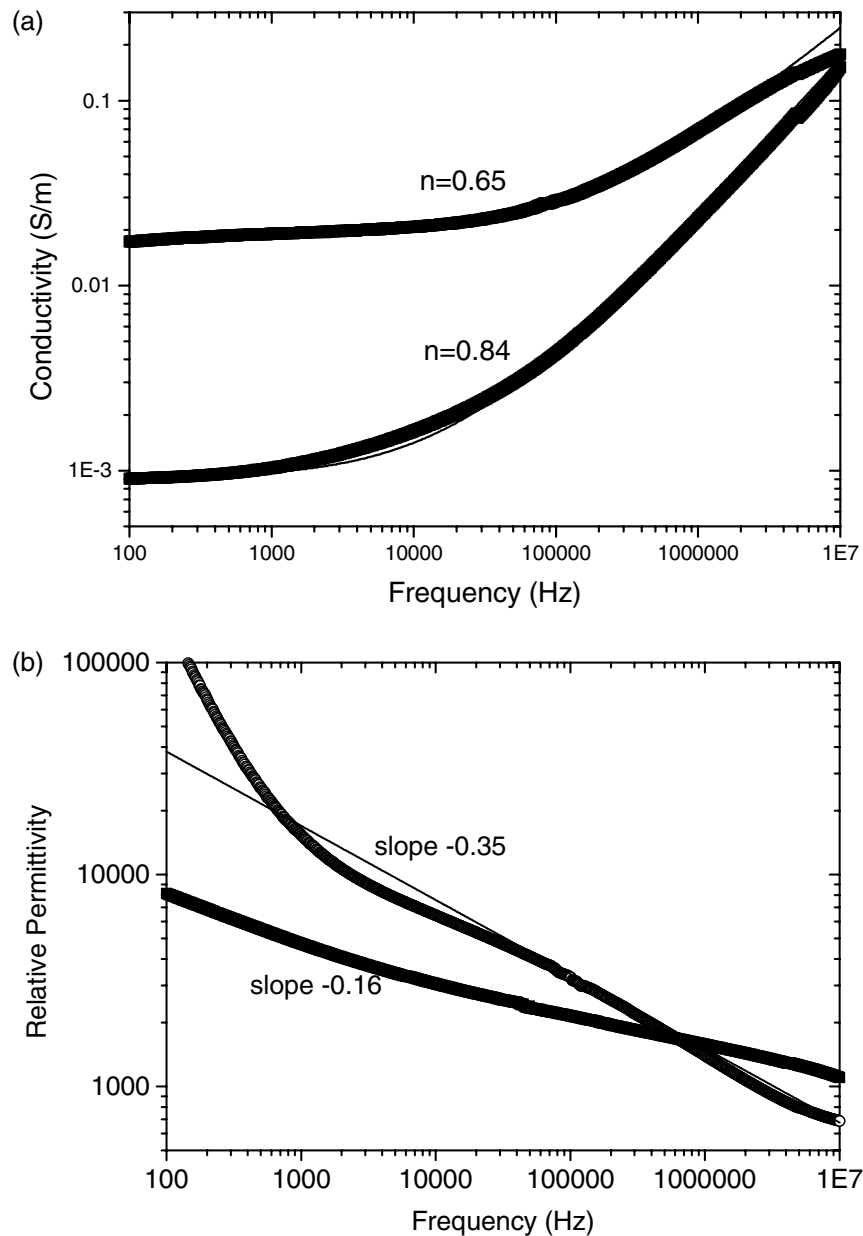


Figure 7. Measurements of (a) the conductivity and (b) the relative permittivity of 16% and 35% porous PZT samples saturated with water.

(figures 3 and 4). The line shown with the data in figure 6(d) was obtained from equation (8), setting $\epsilon = 1500$, the relative permittivity of bulk PZT; $\sigma = 0.13 \text{ Sm}^{-1}$, the water conductivity indicated by the measurements shown in figure 6(b) and $n = 0.78$, the proportion of the sample occupied by PZT, the insulating phase. The slope of the line from equation (8) is $-(1 - n) = -0.22$ i.e. of magnitude equalling the porosity, 22%, of the sample. It can be seen that the agreement between the model line and the data is excellent in both slope and absolute amplitude. The same properties were inserted into equation (7) to calculate the frequency dependence of the ac conductivity. This was added to the percolation plateau value of 0.0048 Sm^{-1} , indicated by the experimental data, to generate the curve shown in figure 6(c). Again the overall agreement between the model curve and the data is excellent.

Similar measurements were made for two further porous PZT samples, one with a lower porosity of 16% and the other with a higher porosity of 35%. The frequency dependences of ac conductivity and relative permittivity are shown in figures 7(a) and (b). The model curves shown with data were generated using the same conductivity and permittivity for the two phases, listed above, with n set as 0.84 and 0.65 for the lower and higher porosity sample cases, respectively. Again the overall agreement between the model curves and the data is excellent. The composition dependence of the permittivity is seen to take the form indicated in figure 5. There is also clear evidence, figure 7(a), that composition determines the exponent for the power law dispersion in ac conductivity. In figure 7(b), the deviation from the predicted power law dispersion at low frequencies for the 65% porous sample is an electrode polarization effect [18]

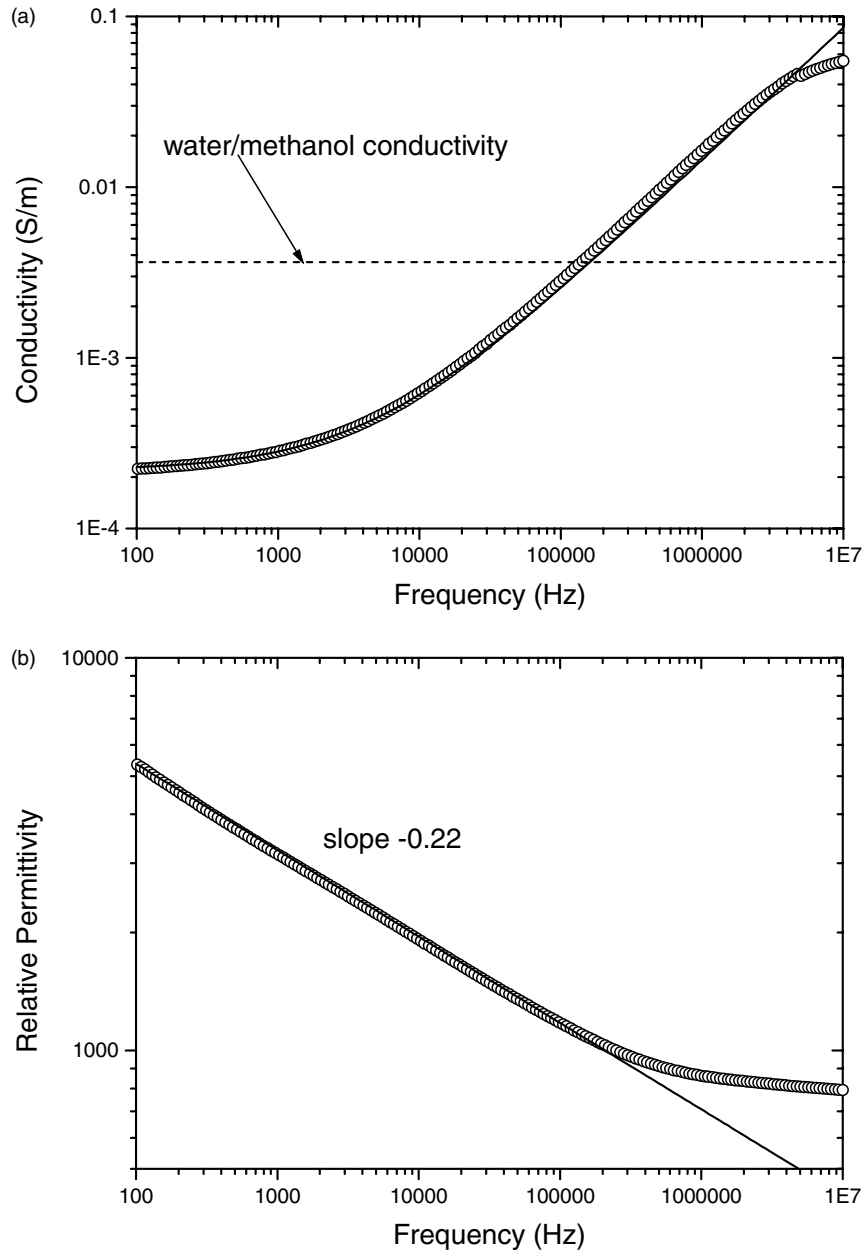


Figure 8. Measurements of (a) the conductivity and (b) the relative permittivity of a 22% porous PZT sample saturated with a solution containing 90% methanol and 10% water.

typical of samples with a high dc ionic conductivity. It is most significant for this sample because, being the sample with the highest porosity, it has the highest dc ionic conductivity.

The water was removed from the 22% porous PZT pellet and its pore volume was refilled with a solution containing 90% methanol and 10% water. This solution had been found to have a conductivity of $3.64 \times 10^{-3} \text{ Sm}^{-1}$, a factor of 35.7 lower than the water used in the tests described above. The frequency dependences of the ac conductivity and relative permittivity of the sample containing the lower conductivity fluid are shown in figures 8(a) and (b). These data should be compared with those shown in figure 6 obtained from the same sample containing water alone. As expected, the

low frequency plateau in conductivity occurs at a much-reduced value of conductivity in figure 8(a). In addition, the power law dispersion in conductivity spans a far greater proportion of the frequency range investigated. This is a result of the characteristic frequency being reduced by the same amount as the conductivity of the conducting phase. The conductivity results in figures 7 and 8 are in good agreement with the modelling predictions for ac conductivity shown in figure 3. The relative permittivity exhibits a slope of -0.22 at low frequencies and a plateau value corresponding to the permittivity of the dry PZT pellet at high frequencies. This is in agreement with the modelling predictions for permittivity shown in figure 4. The curves shown with the data in figure 8 were generated by equations (7) and (8) using the conductivity

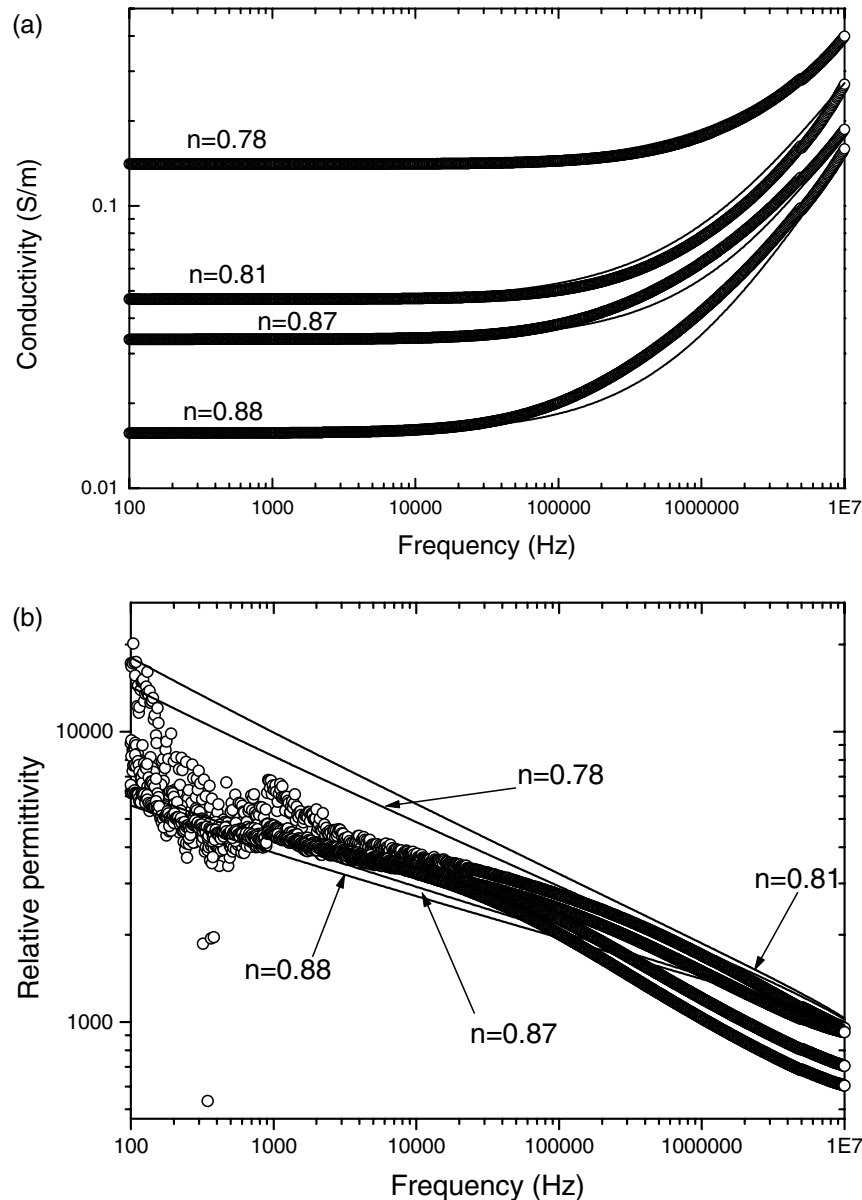


Figure 9. Measurements of (a) the conductivity and (b) the relative permittivity of PZT samples (porosity $1 - n$) impregnated with Panipol CX conducting polymer.

of the solution quoted above. Again the agreement is excellent over most of the frequency range.

Whilst the use of water and other fluids for the conducting phase has many advantages, the composites produced are not stable because they dry out over time. In an effort to produce stable samples, the conducting polymer Panipol CX [19] has been investigated as an alternative conducting phase. Panipol CX was found to have a frequency independent conductivity of 1.5 Sm^{-1} at frequencies up to 10 MHz. Unlike water, it was not possible to infuse the polymer as a liquid into a porous ceramic. Instead granules of Panipol CX and PZT were mixed together and pressed to form a pellet. The ac conductivities and relative permittivities of four PZT Panipol CX samples are shown in figures 9(a) and (b). The lines shown with the data were calculated as before. The agreement between the model curves and the data is reasonable for ac conductivity and poor for relative permittivity. The reason for the poorer agreement,

when compared with using water, was that the polymer fails to completely fill all the spaces between the PZT grains, leaving internal air gaps that have a particularly deleterious effect on measured permittivity.

5. Discussion and conclusions

The experimental studies have shown that simple modelling based on network simulation results provides a comprehensive description of the electrical characteristics of a conductor-insulator composite system across a wide range of frequencies. In particular, equations (7) and (8) which were obtained from the logarithmic mixing rule equation (1), provide an accurate description of the frequency dependent component of a conductor-insulator composite's electrical response characteristics. The use of these expressions was based on the discovery that simulations of large 2D networks of randomly

sited resistors and capacitors exhibited emergent properties that conformed to these expressions. Recent simulations of large 3D networks of randomly sited elements having two different conductivities exhibit essentially identical emergent properties. These results are consistent with expressions obtained from 2D network simulations (equations (7) and (8)), also predicting the properties of real 3D materials. It should be emphasized, however, that materials for which the analysis shown here is relevant are confined to those whose microstructures can be described as being a random array of two phases that are individually conducting and insulating and which occupy volumes that have the same average aspect ratio. If the latter requirement is relaxed, the magnitudes of the frequency dependent expressions, equations (7) and (8), will be altered but the power law frequency dependence and the relationship between the exponents and composition will not be changed.

A simple relationship has been identified between the frequency dependence of relative permittivity and sample porosity/composition. There may be applications for which this relationship will prove to be a valuable means of the assessment of this property.

The physical/mathematical origin of the emergent power law regime found in the 2D and 3D simulations of large networks filled randomly with components of two types is not understood and remains the subject of future research. It appears to be a general characteristic of Laplacian systems that may have widespread application in explaining phenomena in other fields.

References

- [1] Brosseau C and Beroual A 2003 *Prog. Mater. Sci.* **48** 373
- [2] Jonscher A K 1975 *Colloids Polym. Sci.* **253** 231
- [3] Jonscher A K 1983 *Dielectric Relaxations in Solids* (London: Chelsea Dielectric Press)
- [4] Dyre J C and Schroder T B 2000 *Rev. Mod. Phys.* **72** 873
- [5] Almond D P and Bowen C R 2004 *Phys. Rev. Lett.* **92** 157601
- [6] Almond D P and Vainas B 1999 *J. Phys.: Condens. Matter* **11** 9081
- [7] Vainas B, Almond D P, Lou J and Stevens R 1999 *Solid State Ion.* **126** 65
- [8] Bouamrane R and Almond D P 2003 *J. Phys.: Condens. Matter* **15** 4089
- [9] SIMetrix, Newbury Technology Ltd, Thatcham, Berks. RG18 4LZ, UK
- [10] Stauffer D 1985 *Introduction to Percolation Theory* (London: Taylor and Francis) p 17
- [11] Essam J W, Gaunt D S and Guttmann A J 1978 *J. Phys. A: Math. Gen.* **11** 1983
- [12] Lichtenecker K 1926 *Z. Phys.* **27** 115
- [13] Archie G E 1942 *Trans. AIME* **146** 54
- [14] Bowen C R, Perry A, Lewis A C F and Kara H 2004 *J. Eur. Ceram. Soc.* **24** 541
- [15] Smay J E, Cesarano J C, Tuttle B A and Lewis J A 2002 *J. Appl. Phys.* **92** 6119
- [16] Banno H 1993 *Japan. J. Appl. Phys.* **32** 4214
- [17] Bowen C R, Perry A, Kara and Mahon S 2001 *J. Eur. Ceram. Soc.* **21** 1463
- [18] Bauerle J E 1969 *J. Phys. Chem. Solids* **30** 2657
- [19] Panipol Ltd, Työpajatie 20, FIN-06150 Porvoo, Finland
- [20] Panteny S R *PhD Thesis* University of Bath, UK